Supporting Information

Drug-resistance mechanisms of three mutations in anaplastic lymphoma kinase against two inhibitors based on MM/PBSA combined with the interaction entropy

Zhengrong Xiao, [§,1] *Yalong Cong,* [§,2] *Susu Zhong,*[1] *Kaifang Huang,*[1] *John Z. H. Zhang,*[2,3,4] *Lili Duan*[*,1]

[1]School of Physics and Electronics, Shandong Normal University, Jinan, 250014, China

[2]Shanghai Engineering Research Center of Molecular Therapeutics and New Drug Development, School of Chemistry and Molecular Engineering, East China Normal University, Shanghai, 200062, China

[3]NYU-ECNU Center for Computational Chemistry at NYU Shanghai, Shanghai, 200062, China

[4]Department of Chemistry, New York University, NY, NY 10003, USA

Corresponding author (duanll@sdnu.edu.cn)

§Zhengrong Xiao and Yalong Cong contributed equally to this work

1. Analysis of stability of the complexes

The root mean square deviation (RMSD) of the backbone atoms relative to the corresponding X-ray crystal structure was calculated during the whole MD trajectory and used to evaluate the structural stability of complex. As shown in Figure S1 and S2, the simulations of the eight systems (four proteins against two inhibitors) reached equilibrium after approximately 15 ns under either AMBER or PPC force field. The backbone RMSD distributions of these systems were shown in Figures S3 and S4. It was worth noting that RMSD values ranged between 1 to 2.5 Å, which suggested that the MD simulations were converged.

Previous studies also demonstrated that there were lower RMSD values and the more stable structures under PPC force field compared to those from AMBER. In our work, the RMSDs obtained from PPC force field were smaller than those of the AMBER force field, except for the 5P8-L1198F system, where the highest RMSD values from the AMBER and PPC force fields were similar, as shown in Figure S3.

2. Impact of mutations on hydrogen bonds in ALK-5P8 systems

2.1. The hydrogen bonds between ALK and 5P8

In ALK-5P8 systems, there were two main hydrogen bonds between protein and inhibitor, located on residues MET1199 and GLU1197. The length, angle and occupancy of the main hydrogen bonds under the AMBER and PPC force fields were computed and listed in Table S1. The hydrogen bond was defined as angle greater than

120 degrees and distance between two heavy atoms of less than 3.5 Å. In ALK-5P8 systems, it was obvious that the occupancies of hydrogen bonds were primarily higher in PPC than AMBER, especially the hydrogen bond between GLU1197 and inhibitor. This indicated that the polarization had a significant effect on stabilizing hydrogen bonds. The following analyses were based on the results from PPC.

In ALK-5P8 systems, the hydrogen bonds between MET1199 residue and the inhibitor were slightly unstable in the L1189F and C1156Y/L1198F systems, with occupancies of 96.40% and 94.90%, respectively. The hydrogen bond was dominated by electrostatic interactions, and strong electrostatic interaction was helpful in stabilizing the hydrogen bond. The result was in good agreement with the analysis of the binding free energy, in which the electrostatic interaction was stronger in the WT and C1156Y systems than in the L1198F and C1156Y/L1188F systems, as seen in Table 1(A). The hydrogen bond formed between the GLU1197 residue and the inhibitor was very stable in the four systems with an occupancy of above 99% in each system. From the above analysis, the hydrogen bond formed between MET1199 and 5P8 had an important impact on the L1198F mutation, which resulted in the weak binding free energy in the L1198F and C1156Y/L1198F mutations. The other hydrogen bond had almost no effect on the three mutation systems.

2.2. The intramolecular hydrogen bonds in ALK protein

The intramolecular hydrogen bonds connected with the mutated residues in ALK-5P8 systems were further analyzed and those results were listed in Table S2. In Table S2, it can be observed that the 1156 residue can form a hydrogen bond with ALA1126

after being mutated into tyrosine. It was shown in Figure S5. Besides, in Table S2, the occupancies of ALA1126-TYR1156 hydrogen bond in the C1156Y (29.89%) and C1156Y/L1198F (83.23%) mutation systems indicated that the L1198F mutation can stabilize the hydrogen bond. Moreover, one point can be found from the Table S2 that the occurrence of C1156Y mutation led to a decrease in occupancy of hydrogen bond between the 1198 residue and ALA1200. These results were further discussed in the following section.

3. Impact of mutations on RMSF in ALK-5P8 systems

The root-mean-square fluctuation (RMSF) of the Cα atoms in ALK-5P8 systems was calculated using the equilibrated trajectories from the PPC force field for furtherly investigating the conformational change induced by residue mutation. As shown in Figure S6, the decreased RMSF around GLY1125 and VAL1155 in C1156Y and C1156Y/L1198F mutation systems showed that the C1156Y mutation had an important influence on stabilizing the region surrounding GLY1125 and Val1155 residues. This was because no hydrogen bond was formed between ALA1126 and TYR1156 before the 1156 residue was mutated to tyrosine. The hydrogen bond between ALA1126 and TYR1156 in the C1156Y and C1156Y/L1198F mutation systems could stabilize the structure and decrease the RMSF values of the surrounding residues, as shown in Figure S5. In addition, the RMSF values of residues near SER1333 and SER1344 were increased in the C1156Y mutation, which demonstrated that this region had higher flexibility after mutation than WT. While, the RMSF values of this region were lower in the L1198F and C1156Y/L1198F system than C1156Y system, which showed that

the L1198F mutation could weaken the amplified flexibility caused by the C1156Y mutation.

4. Impact of mutations on hydrogen bonds in ALK-VGH systems

4.1. The hydrogen bonds between ALK and VGH

As ALK-5P8 systems, there were two main hydrogen bonds between protein and inhibitor in ALK-VGH systems, located on residues MET1199 and GLU1197. Detailed results of length, angle and occupancy of the hydrogen bonds in ALK-VGH complexes under the AMBER and PPC force fields were displayed in Table S3. From Table S3, the occupancies of the hydrogen bonds were high (greater than 99%) in both AMBER and PPC. Compared with 5P8, those hydrogen bonds formed with VGH were more stable, which corresponded with the higher electrostatic interaction shown in Table 3 (A) than in Table 1 (A). In the GLU1197O-inhibitor H8/H9-N1 hydrogen bond, the H8 and H9 atoms in the inhibitor were exchanged frequently in the C1156Y system, as shown in Figure S7. All hydrogen bonds were quite stable in the four systems, which can be explained form the stronger electrostatic interaction in the ALK-VGH than ALK-5P8 systems. The hydrogen bonds were dominated by electrostatic interaction, and the inhibitor VGH had one positive charge compared with the neutral 5P8. This explained the higher occupancies of hydrogen bonds in ALK-VGH than ALK-5P8 systems.

4.2. The intramolecular hydrogen bonds in ALK protein

The intramolecular hydrogen bonds connected with the mutated residues in ALK-VGH systems were further analyzed and those results were listed in Table S4. In Table S4, ALA1126 could establish hydrogen bonds after the 1156 residue mutates into tyrosine, but it was weakened in the C1156Y/L1198F mutation compared to the C1156Y mutation, with occupancies of 33.53% and 58.98%, respectively. While in ALK-5P8 systems, the occupancy of this hydrogen bond was increased in the C1156Y/L1198F system. This difference of occupancy change induced the conformational change difference between ALK-5P8 and ALK-VGH systems.

5. Impact of mutations on RMSF in ALK-VGH systems

The RMSF of the Cα atoms in ALK-VGH systems was calculated using the equilibrated trajectories from the PPC force field. In Figure S8, the RMSF values of the residues around ALA1126 were decreased in all mutation types, and the RMSF values of GLY1287 were decreased in the C1156Y and C1156Y/L1198F mutations, which indicated that the C1156Y mutation could stabilize the region surrounding GLY1287 residue. In the ALK-VGH systems, the L1198F mutation could stabilize the N-terminal lobe. Comparing with ALK-5P8 systems, the conformation change of same mutation type was obviously different, which was induced by the difference of inhibitors. The structure of VGH was more flexible than 5P8, which provided different structure change in the same mutation types. Detailed analyses about inhibitors are shown on section Differences between the two inhibitors in the manuscript.

Tables

Table S1. Main hydrogen bonds interactions of 5P8 with the WT/mutated ALK.

Mutation	Acceptor	Donor	AMBER			PPC		
			Angle (°)	Distance (Å)	Occupancy (%)	Angle (°)	Distance (Å)	Occupancy (%)
WT	InhibitorN2	MET1199N-H	153.73	3.13	97.01	153.48	2.94	99.78
	GLU1197O	InhibitorN6-H19	161.12	2.98	27.23	164.96	2.85	99.88
C1156Y	InhibitorN2	MET1199N-H	157.55	3.07	99.13	152.5	2.99	99.72
	GLU1197O	InhibitorN6-H19	159.32	2.97	98.84	163.95	2.84	99.98
L1198F	InhibitorN2	MET1199N-H	151.39	3.26	77.65	148.95	3.14	96.40
	GLU1197O	InhibitorN6-H19	160.64	2.97	44.10	165.63	2.91	99.58
C1156Y/L1198F	InhibitorN2	MET1199N-H	150.80	3.27	72.60	146.53	3.14	94.90
	GLU1197O	InhibitorN6-H19	161.33	3.08	87.55	165.78	2.90	99.55

Table S2. Main hydrogen bonds interactions of residue CYS/TYR1156 and LEU/PHE1198 with the WT/mutated ALK in ALK-5P8 systems.

The hydrogen bond	Mutation	Angle (°)	Distance (Å)	Occupancy （%）
ALA1126O-TYR1156HH-OH	WT	NA	NA	NA
	C1156Y	159.32	2.78	29.89
	L1198F	NA	NA	NA
	C1156Y/L1198F	159.23	2.75	83.23
LEU/PHE1198O-ALA1200H-N	WT	132.91	2.94	72.39
	C1156Y	129.86	2.98	45.50
	L1198F	134.30	3.00	73.42
	C1156Y/L1198F	132.57	2.98	66.72

Table S3. Main hydrogen bonds interactions of VGH with the WT/mutated ALK.

Mutation	Acceptor	Donor	AMBER			PPC		
			Angle (°)	Distance (Å)	Occupancy (%)	Angle (°)	Distance (Å)	Occupancy (%)
WT	InhibitorN2	MET1199N-H	157.24	3.03	99.35	155.73	2.99	99.18
	GLU1197O	InhibitorN1-H11	164.15	2.95	99.26	165.16	2.81	100.00
C1156Y	InhibitorN2	MET1199N-H	154.00	3.06	98.80	157.38	2.92	99.85
	GLU1197O	InhibitorN1-H8/H9	164.20	2.90	99.84	163.41	2.88	99.90
L1198F	InhibitorN2	MET1199N-H	161.37	3.00	99.85	161.51	2.93	99.93
	GLU1197O	InhibitorN1-H9	164.17	2.98	99.14	165.24	2.84	99.99
C1156Y/L1198F	InhibitorN2	MET1199N-H	161.88	3.01	99.88	160.88	2.93	99.93
	GLU1197O	InhibitorN1-H9	163.95	2.91	99.89	164.94	2.89	99.91

Table S4. Main hydrogen bonds interactions of residue CYS/TYR1156 and LEU/PHE1198 with the WT/mutated ALK in VGH-ALK systems.

The hydrogen bond	Mutation	Angle (°)	Distance (Å)	Occupancy（%）
ALA1126O-TYR1156HH-OH	WT	NA	NA	NA
	C1156Y	160.86	2.69	58.98
	L1198F	NA	NA	NA
	C1156Y/L1198F	159.29	2.75	33.53
LEU/PHE1198O-ALA1200H-N	WT	128.61	3.04	14.31
	C1156Y	131.28	3.09	57.25
	L1198F	127.90	3.09	16.97
	C1156Y/L1198F	128.33	3.11	28.15

Table S5. The value and standard error of predicted hot-spot residues entropy, the enthalpy of side chain and backbone part in predicted hot-spot residues, total energy of every residue and the sum in every system in ALK-5P8 systems.

Mutant Types	*Predicted hot-sot residues*	*-TΔS*	*Side chain*	*Backbone*	*Total Energy*	
WT	LEU1122	1.10±0.00	-5.08±0.09	0.56±0.10	-3.42	-24.87
	Val1133	0.55±0.00	-2.62±0.08	-0.10±0.01	-2.17	
	GLU1197	2.32±0.00	-0.10±0.01	-4.80±0.12	-2.58	
	LEU/PHE1198	0.69±0.00	-2.58±0.09	-2.60±0.06	-4.49	
	MET1199	2.24±0.00	-2.14±0.09	-5.80±0.15	-5.70	
	GLY1202	0.34±0.00	-1.04±0.03	-1.66±0.07	-2.36	
	LEU1256	1.24±0.00	-5.14±0.13	-0.14±0.01	-4.04	
C1156Y	LEU1122	1.03±0.00	-4.86±0.10	0.20±0.06	-3.63	-25.36
	Val1133	0.70±0.00	-3.12±0.08	-0.14±0.01	-2.56	
	GLU1197	2.09±0.00	-0.14±0.01	-4.30±0.15	-2.35	
	LEU/PHE1198	0.98±0.00	-2.84±0.08	-2.50±0.05	-4.36	
	MET1199	2.86±0.00	-2.14±0.05	-5.52±0.14	-4.80	
	GLY1202	0.39±0.00	-1.18±0.05	-1.78±0.09	-2.57	
	LEU1256	1.29±0.00	-6.16±0.11	-0.22±0.01	-5.09	
L1198F	LEU1122	0.99±0.00	-4.36±0.12	0.06±0.08	-3.31	-19.01
	Val1133	1.10±0.00	-3.64±0.14	-0.18±0.01	-2.72	
	GLU1197	4.33±0.00	-0.08±0.01	-4.06±0.14	0.19	
	LEU/PHE1198	0.58±0.00	-1.54±0.07	-1.78±0.05	-2.74	
	MET1199	2.56±0.00	-1.76±0.09	-4.34±0.11	-3.54	
	GLY1202	0.34±0.00	-0.94±0.04	-1.88±0.06	-2.48	
	LEU1256	1.83±0.00	-5.98±0.14	-0.22±0.01	-4.37	
C1156Y/L1198F	LEU1122	1.66±0.00	-4.94±0.12	0.16±0.06	-3.12	-21.48
	Val1133	0.52±0.00	-3.22±0.09	-0.20±0.01	-2.90	
	GLU1197	2.92±0.00	-0.08±0.02	-4.40±0.18	-1.56	
	LEU/PHE1198	0.76±0.00	-1.50±0.07	-1.60±0.05	-2.34	
	MET1199	2.95±0.00	-1.88±0.10	-4.24±0.15	-3.17	
	GLY1202	0.28±0.00	-1.10±0.05	-1.94±0.07	-2.76	
	LEU1256	1.11±0.00	-6.42±0.12	-0.26±0.01	-5.57	

Table S6. The backbone and side chain contribution of predicted hot-spot residues in ALK-5P8 systems.

Predicted Hot-spot residues	*Mutants*	ΔE_{vdw}		ΔE_{ele}		ΔG_{pol}		ΔG_{nopol}	
		Side chain	*Backbone*	*Side chain*	*Backbone*	*Side chain*	*Backbone*	*Side chain*	*Backbone*
LEU1122	WT	-4.62±0.09	-0.68±0.07	0.00±0.04	-1.94±0.08	0.22±0.03	3.28±0.09	-0.68±0.01	-0.08±0.01
	C1156Y	-4.36±0.10	-0.88±0.04	-0.28±0.03	-1.38±0.07	0.44±0.03	2.64±0.09	-0.66±0.01	-0.16±0.01
	L1198F	-3.98±0.11	-1.00±0.07	0.00±0.03	-1.26±0.07	0.22±0.02	2.54±0.10	-0.60±0.02	-0.22±0.01
	C1156Y/L1198F	-4.40±0.11	-0.86±0.04	-0.18±0.03	-0.86±0.09	0.40±0.02	2.06±0.12	-0.74±0.01	-0.18±0.01
Val1130	WT	-2.18±0.07	-0.18±0.00	0.14±0.03	-0.46±0.04	-0.26±0.02	0.56±0.03	-0.32±0.01	0.00±0.00
	C1156Y	-2.58±0.08	-0.22±0.01	0.26±0.03	-0.76±0.04	-0.36±0.03	0.82±0.03	-0.44±0.01	0.00±0.00
	L1198F	-3.14±0.14	-0.30±0.01	0.14±0.03	-0.54±0.04	-0.04±0.02	0.66±0.04	-0.58±0.01	0.00±0.00
	C1156Y/L1198F	-2.66±0.09	-0.24±0.01	0.40±0.04	-0.90±0.04	-0.46±0.03	0.96±0.04	-0.50±0.01	0.00±0.00
GLU1197	WT	-0.38±0.01	0.68±0.18	1.32±0.08	-7.80±0.26	-1.04±0.08	2.34±0.10	0.00±0.00	-0.02±0.00
	C1156Y	-0.40±0.01	0.64±0.19	1.46±0.09	-7.30±0.29	-1.20±0.08	2.40±0.10	0.00±0.00	-0.02±0.00
	L1198F	-0.34±0.01	0.18±0.15	1.14±0.07	-6.48±0.30	-0.88±0.07	2.28±0.11	0.00±0.00	-0.04±0.00
	C1156Y/L1198F	-0.40±0.01	0.12±0.16	1.34±0.08	-6.86±0.37	-1.02±0.08	2.36±0.11	0.00±0.00	-0.02±0.00
LEU/PHE1198	WT	-2.10±0.08	-1.12±0.02	-1.86±0.05	-2.36±0.08	1.50±0.03	0.88±0.05	-0.10±0.01	0.00±0.00
	C1156Y	-2.18±0.07	-1.14±0.02	-2.12±0.05	-2.14±0.08	1.58±0.03	0.78±0.05	-0.12±0.01	0.00±0.00
	L1198F	-1.70±0.08	-0.86±0.02	-0.72±0.06	-1.80±0.07	0.98±0.03	0.88±0.05	-0.08±0.01	0.00±0.00
	C1156Y/L1198F	-1.46±0.06	-0.86±0.02	-1.12±0.07	-1.08±0.07	1.20±0.04	0.34±0.05	-0.14±0.01	0.00±0.00
MET1199	WT	-1.66±0.09	-0.38±0.17	-2.18±0.05	-9.12±0.27	1.72±0.03	3.84±0.11	-0.02±0.00	-0.14±0.00
	C1156Y	-1.84±0.06	-0.50±0.17	-1.48±0.05	-8.54±0.28	1.20±0.03	3.64±0.11	0.00±0.00	-0.12±0.00
	L1198F	-1.50±0.10	-1.54±0.11	-0.98±0.04	-5.88±0.22	0.74±0.03	3.26±0.11	-0.02±0.00	-0.18±0.00
	C1156Y/L1198F	-1.46±0.12	-1.40±0.10	-1.64±0.06	-5.48±0.26	1.22±0.03	2.80±0.11	-0.02±0.00	-0.14±0.00
GLY1202	WT	-0.86±0.02	-1.62±0.05	-0.96±0.06	1.22±0.10	0.82±0.04	-0.92±0.07	-0.04±0.00	-0.34±0.01
	C1156Y	-1.00±0.03	-1.86±0.06	-1.14±0.09	1.48±0.12	1.00±0.06	-1.06±0.08	-0.04±0.00	-0.34±0.01
	L1198F	-0.90±0.03	-1.72±0.05	-0.74±0.06	0.98±0.09	0.72±0.05	-0.82±0.07	-0.04±0.00	-0.32±0.01
	C1156Y/L1198F	-1.06±0.02	-1.98±0.04	-1.00±0.09	1.22±0.14	0.98±0.07	-0.86±0.10	-0.04±0.00	-0.32±0.01
LEU1256	WT	-4.66±0.13	-0.18±0.01	-0.14±0.05	-0.20±0.03	0.32±0.04	0.24±0.03	-0.66±0.01	0.00±0.00
	C1156Y	-5.64±0.11	-0.26±0.01	-0.42±0.04	-0.12±0.03	0.50±0.03	0.16±0.02	-0.58±0.01	0.00±0.00
	L1198F	-5.40±0.14	-0.26±0.01	-0.36±0.05	-0.10±0.03	0.38±0.04	0.14±0.03	-0.62±0.01	0.00±0.00
	C1156Y/L1198F	-5.86±0.12	-0.32±0.01	-0.34±0.04	-0.24±0.03	0.34±0.04	0.30±0.03	-0.58±0.01	0.00±0.00

Table S7. The value and standard error of predicted hot-spot residues entropy, the enthalpy of side chain and backbone part in predicted hot-spot residues, total energy of every residue and the sum in every system in ALK-VGH systems.

Mutant Types	***Predicted hot-sot residues***	***-TΔS***	***Side chain***	***Backbone***	***Total Energy***	
WT	LEU1122	1.72±0.00	-4.22±0.15	0.08±0.05	-2.42	-15.16
	GLU1197	2.78±0.00	-0.38±0.01	-3.50±0.14	-1.10	
	LEU/PHE1198	0.74±0.00	-1.96±0.06	-2.34±0.07	-3.56	
	MET1199	4.94±0.00	-2.04±0.05	-4.44±0.15	-1.54	
	GLY1202	1.36±0.00	-0.70±0.07	-2.72±0.14	-2.06	
	LEU1256	1.56±0.00	-5.74±0.13	-0.30±0.01	-4.48	
C1156Y	LEU1122	1.27±0.00	-4.34±0.11	-0.34±0.06	-3.41	-15.37
	GLU1197	3.24±0.00	-0.40±0.01	-2.94±0.15	-0.10	
	LEU/PHE1198	0.58±0.00	-1.88±0.08	-2.54±0.06	-3.84	
	MET1199	4.26±0.00	-2.78±0.08	-4.36±0.17	-2.88	
	GLY1202	1.79±0.00	-0.76±0.05	-2.50±0.13	-1.47	
	LEU1256	1.09±0.00	-4.56±0.13	-0.20±0.01	-3.67	
L1198F	LEU1122	0.94±0.00	-4.32±0.10	-0.48±0.04	-3.86	-19.75
	GLU1197	2.08±0.00	-0.38±0.01	-3.64±0.13	-1.94	
	LEU/PHE1198	1.11±0.00	-3.76±0.09	-2.20±0.06	-4.85	
	MET1199	3.15±0.00	-2.40±0.04	-4.24±0.15	-3.49	
	GLY1202	1.70±0.00	-0.50±0.05	-3.26±0.13	-2.06	
	LEU1256	1.79±0.00	-5.02±0.13	-0.32±0.01	-3.55	
C1156Y/L1198F	LEU1122	0.96±0.00	-4.88±0.09	-0.24±0.02	-4.16	-19.90
	GLU1197	2.12±0.00	-0.34±0.01	-3.90±0.10	-2.12	
	LEU/PHE1198	1.11±0.00	-3.50±0.11	-2.22±0.05	-4.61	
	MET1199	3.10±0.00	-2.38±0.05	-3.96±0.13	-3.24	
	GLY1202	1.58±0.00	-0.38±0.08	-3.40±0.13	-2.20	
	LEU1256	1.29±0.00	-4.60±0.12	-0.26±0.01	-3.57	

Table S8. The backbone and side chain contribution of predicted hot-spot residues in ALK-VGH systems.

Predicted Hot-spot residues	*Mutants*	ΔE_{vdw}		ΔE_{ele}		ΔG_{pol}		ΔG_{nopol}	
		Side chain	*Backbone*	*Side chain*	*Backbone*	*Side chain*	*Backbone*	*Side chain*	*Backbone*
LEU1122	WT	-3.60±0.14	-0.66±0.05	-8.44±0.17	5.90±0.16	8.56±0.15	-5.00±0.14	-0.72±0.02	-0.16±0.02
	C1156Y	-3.86±0.11	-1.08±0.07	2.82±0.09	-4.18±0.19	-2.68±0.08	5.16±0.20	-0.62±0.02	-0.26±0.02
	L1198F	-3.90±0.10	-0.54±0.02	-1.04±0.04	1.46±0.04	1.18±0.03	-1.40±0.04	-0.56±0.01	0.00±0.00
	C1156Y/L1198F	-4.34±0.09	-0.68±0.04	2.70±0.06	-4.02±0.13	-2.50±0.06	4.62±0.15	-0.74±0.01	-0.14±0.01
GLU1197	WT	-0.44±0.01	1.14±0.20	-14.18±0.17	-12.00±0.28	14.24±0.16	7.40±0.09	0.00±0.00	-0.02±0.00
	C1156Y	-0.34±0.01	0.30±0.18	-14.30±0.14	-10.98±0.29	14.22±0.14	7.74±0.08	0.00±0.00	-0.02±0.00
	L1198F	-0.38±0.01	0.30±0.16	-14.96±0.12	-11.78±0.26	14.96±0.11	7.86±0.08	0.00±0.00	-0.02±0.00
	C1156Y/L1198F	-0.30±0.01	0.20±0.17	-13.74±0.10	-12.42±0.24	13.70±0.10	8.34±0.07	0.00±0.00	-0.02±0.00
LEU/PHE1198	WT	-1.54±0.28	-0.86±0.12	4.20±0.68	-6.98±0.90	-4.52±0.62	5.50±0.80	-0.08±0.06	0.00±0.00
	C1156Y	-1.66±0.40	-0.88±0.08	3.08±0.40	-5.92±0.62	-3.24±0.38	4.26±0.44	-0.04±0.04	0.00±0.00
	L1198F	-3.20±0.50	-0.84±0.10	4.76±0.46	-7.52±0.62	-5.08±0.38	6.16±0.50	-0.24±0.06	0.00±0.00
	C1156Y/L1198F	-3.04±0.54	-0.80±0.22	3.60±0.54	-6.38±0.54	-3.84±0.42	4.96±0.50	-0.24±0.08	0.00±0.00
MET1199	WT	-2.00±0.26	-0.60±0.98	1.16±0.50	-13.58±2.26	-1.20±0.42	9.90±1.52	-0.08±0.00	-0.16±0.01
	C1156Y	-2.46±0.54	-0.10±1.34	1.64±0.62	-14.96±2.08	-1.88±0.42	10.84±1.40	-0.06±0.04	-0.14±0.00
	L1198F	-2.12±0.30	-0.02±1.36	1.44±0.42	-15.50±1.76	-1.70±0.32	11.40±1.00	-0.02±0.02	-0.12±0.00
	C1156Y/L1198F	-2.04±0.34	-0.28±1.06	2.08±0.42	-14.10±1.70	-2.42±0.30	10.52±1.00	-0.02±0.02	-0.12±0.00
GLY1202	WT	-1.00±0.14	-1.62±0.50	-14.14±1.42	14.12±2.06	14.44±1.24	-14.96±1.68	-0.02±0.02	-0.26±0.01
	C1156Y	-0.94±0.16	-1.64±0.44	-14.74±1.60	14.98±2.04	14.94±1.28	-15.54±1.64	-0.02±0.02	-0.32±0.00
	L1198F	-1.06±0.14	-1.82±0.46	-16.66±1.26	16.16±1.86	17.24±1.00	-17.28±1.50	-0.02±0.02	-0.34±0.00
	C1156Y/L1198F	-0.92±0.28	-1.64±0.46	-16.42±1.34	16.74±1.78	17.00±1.10	-18.16±1.40	-0.04±0.02	-0.34±0.00
LEU1256	WT	-5.20±0.86	-0.28±0.04	7.36±0.40	-6.50±0.32	-7.22±0.42	6.46±0.30	-0.68±0.04	0.00±0.00
	C1156Y	-4.20±0.78	-0.16±0.02	6.16±0.42	-4.70±0.22	-5.84±0.42	4.64±0.22	-0.66±0.06	0.00±0.00
	L1198F	-4.66±0.84	-0.26±0.06	6.92±0.34	-5.82±0.24	-6.70±0.34	5.76±0.24	-0.56±0.06	0.00±0.00
	C1156Y/L1198F	-4.20±0.74	-0.18±0.04	6.22±0.42	-5.04±0.22	-6.04±0.38	4.98±0.22	-0.58±0.04	0.00±0.00

Figures

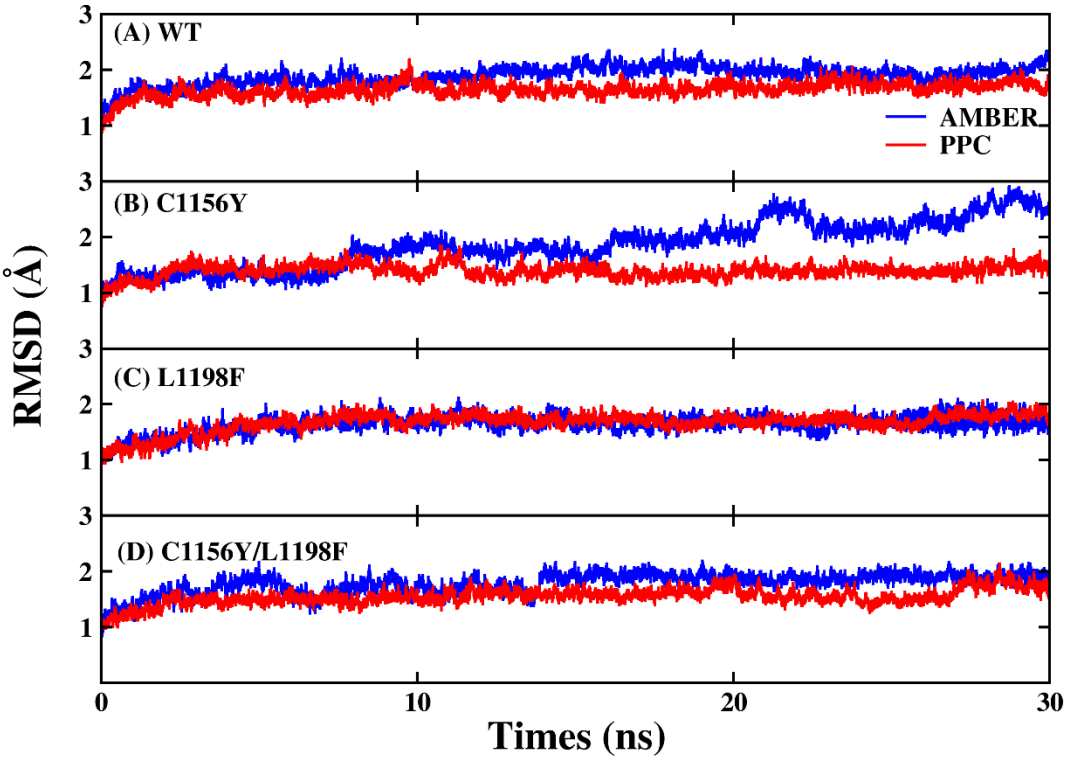

Figure S1. The root-mean-square deviation (RMSD) of the backbone atoms relative to the corresponding native structure in ALK-5P8 system. (A) the wild-type (B) C1156Y (C) L1198F (D) double mutant C1156Y/L1198F

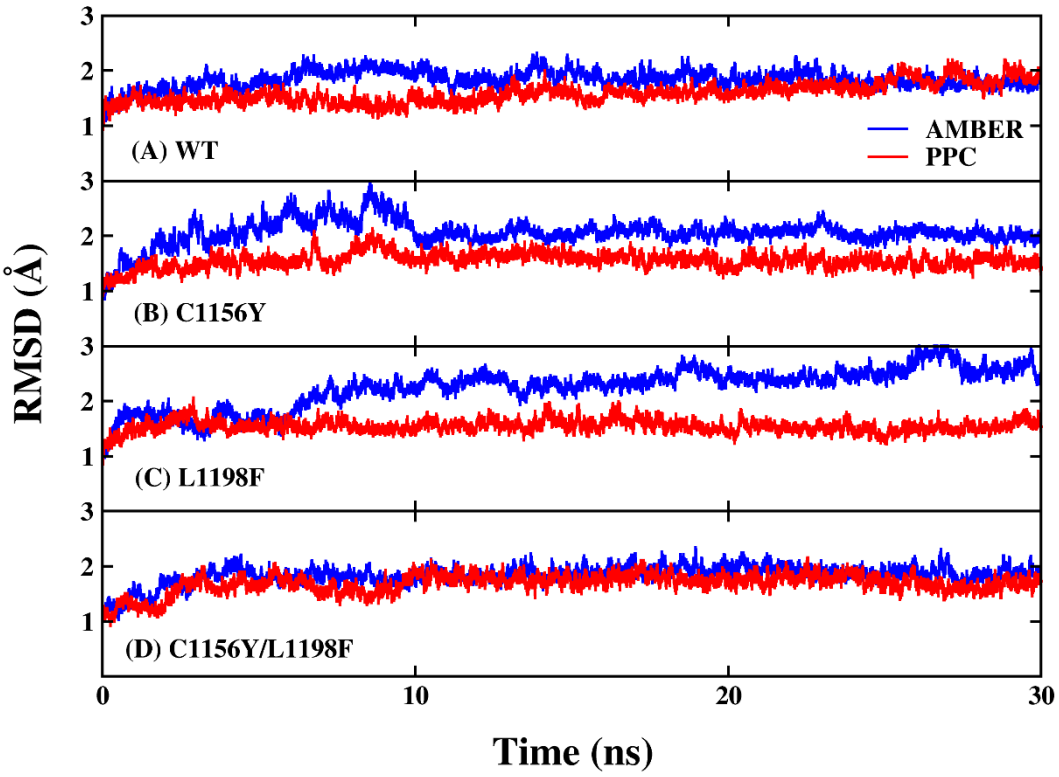

Figure S2. The root-mean-square deviation (RMSD) of the backbone atoms relative to the corresponding native structure in ALK-VGH system. (A) the wild-type (B) C1156Y (C) L1198F (D) double mutant C1156Y/L1198F

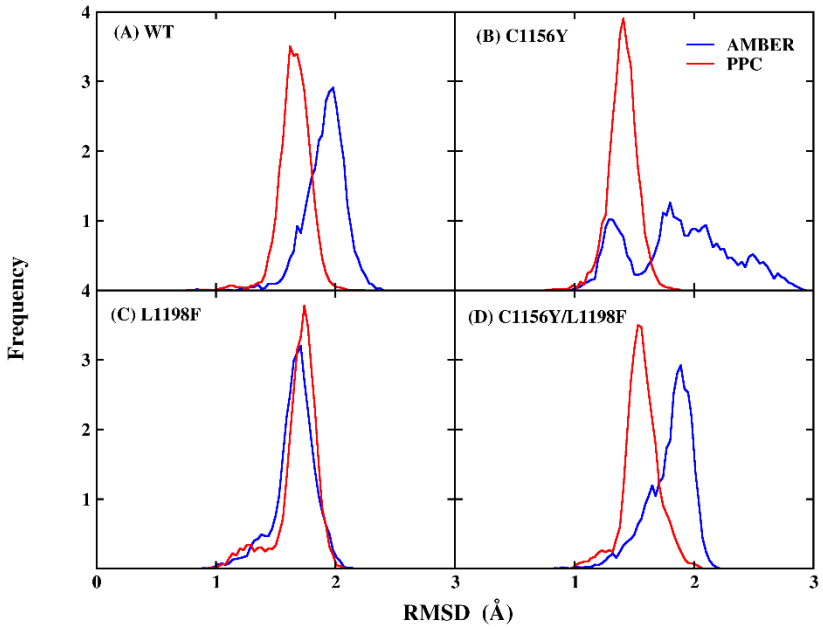

Figure S3. Distribution of backbone RMSD in 5P8 systems under AMBER (blue curve) and PPC (red curve) force field.

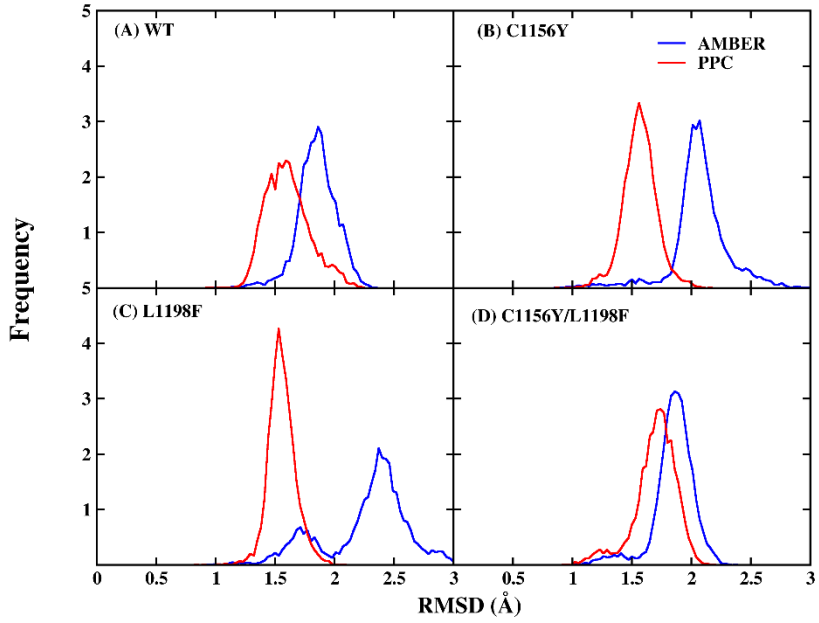

Figure S4. Distribution of backbone RMSD in VGH systems under AMBER (blue curve) and PPC (red curve) force field.

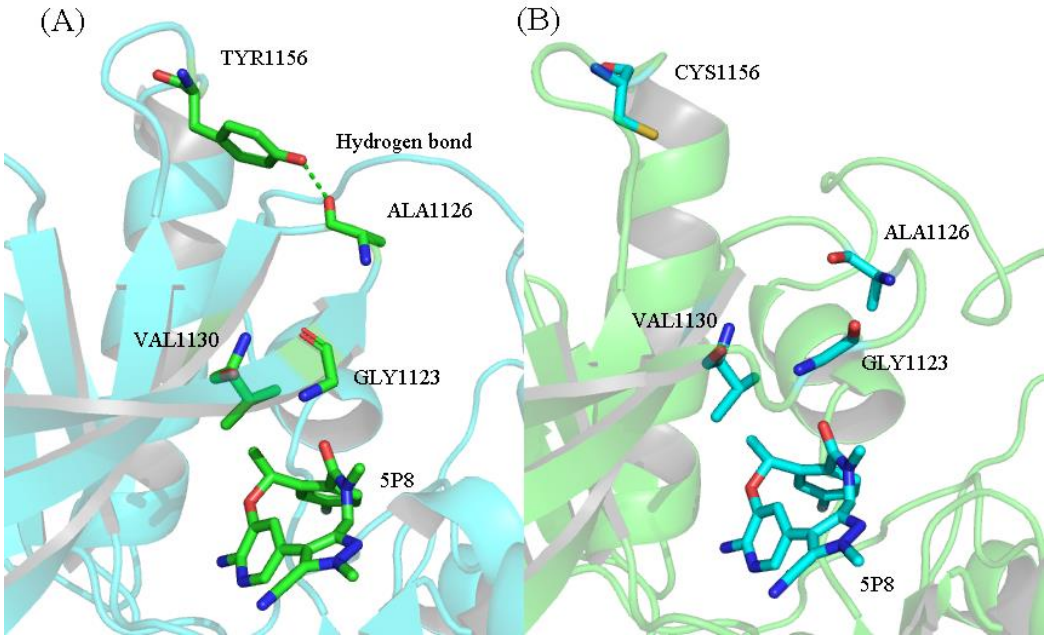

Figure S5. (A) The lowest potential energy structure of C1156Y mutant with 5P8. (B) The lowest potential energy structure of WT with 5P8.

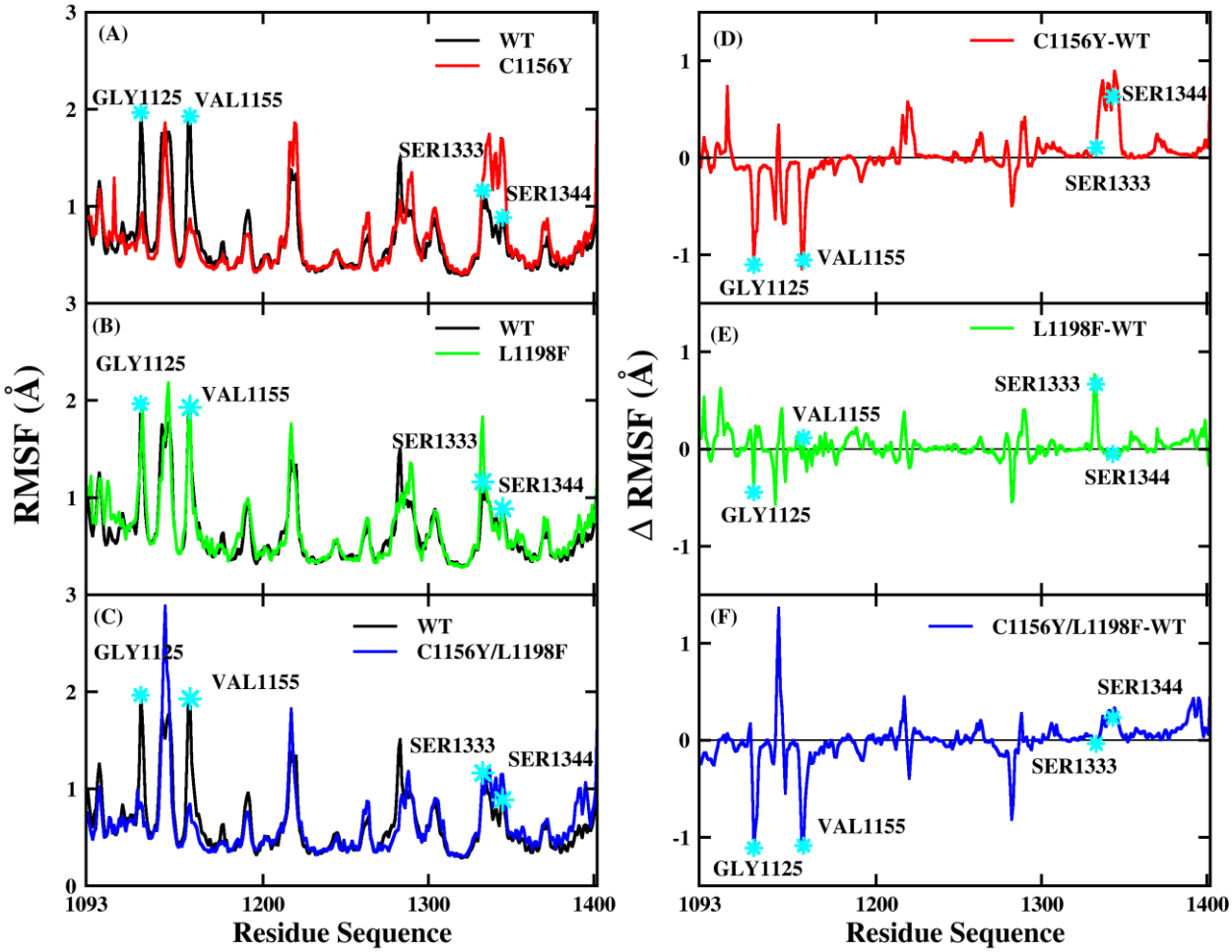

Figure S6. The RMSF of C_α in (A) wild-type and C11156Y, (B) wild-type and L1198F, (C) wild-type and double mutation, and difference of value in (D) wild-type and C11156Y, (E) wild-type and L1198F, (F) wild-type and double mutation in ALK-5P8 systems.

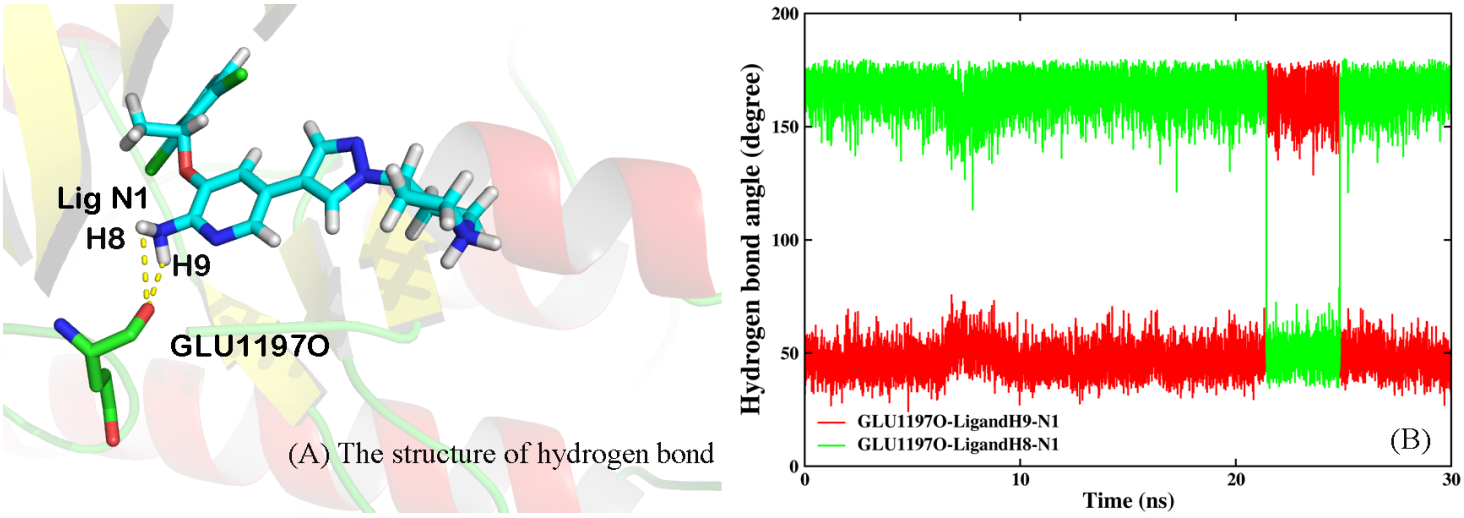

Figure S7. (A) The structure of hydrogen bond GLU1197O-inhibitorH8/H9-N1 in C1156Y to VGH. (B) The angle of hydrogen bond during the simulation.

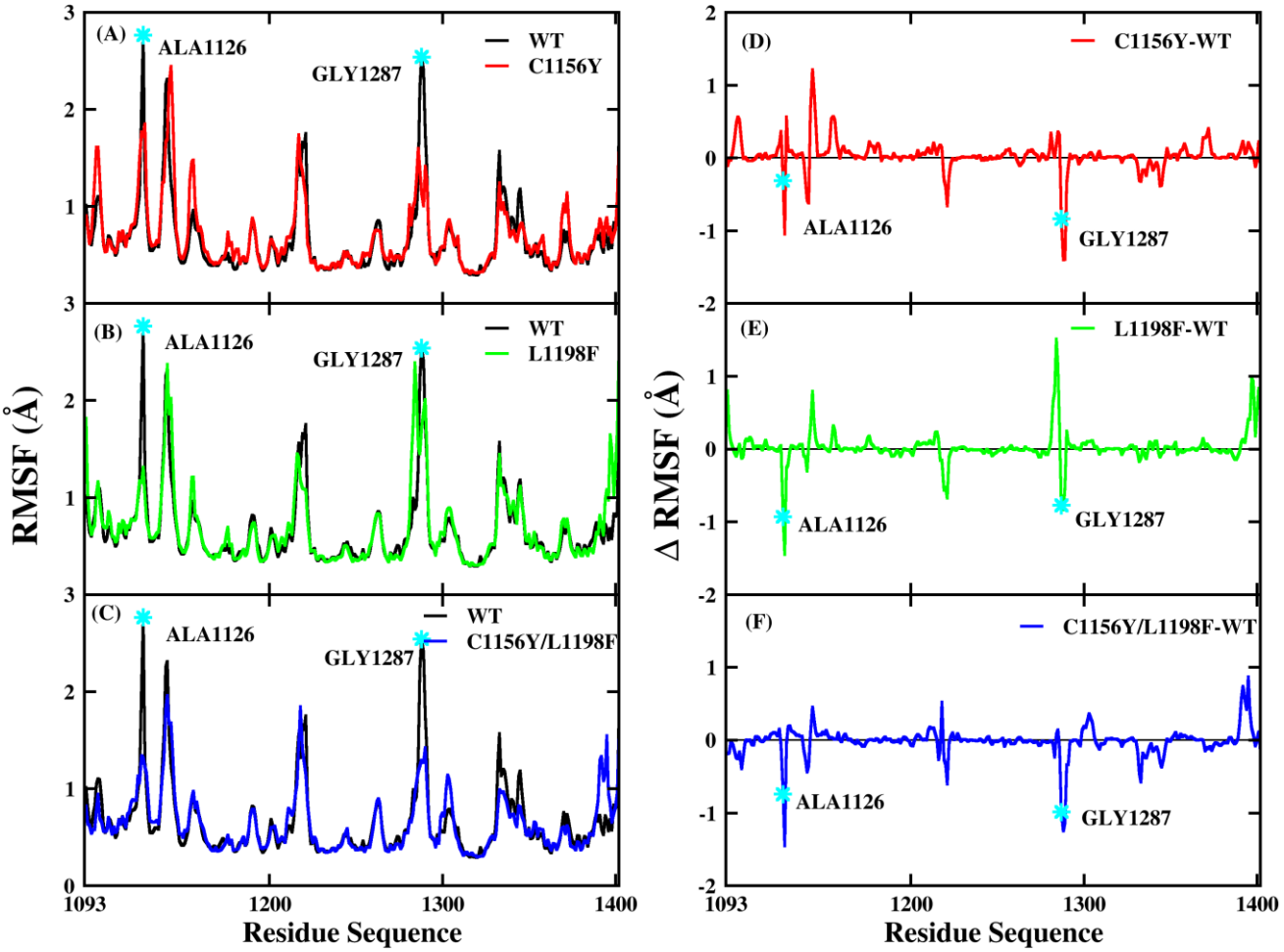

Figure S8. The RMSF of C_α in (A) wild-type and C11156Y, (B) wild-type and L1198F, (C) wild-type and double mutation, and difference of value in (D) wild-type and C11156Y, (E) wild-type and L1198F, (F) wild-type and double mutation in ALK-VGH systems.